Designing and Building a Ski Binding Tester

Project Number: 192806

A Major Qualifying Project Report

Submitted to the Faculty of

Worcester Polytechnic Institute

In partial fulfilment of the requirements for the

Degree of Bachelor of Science

In Mechanical Engineering

By

Jesse Kablik Frank Kinzie

Date: 1/8/17

Keywords:

1. Ski
2. Binding
3. Tester

Approved:

_____

Prof. Christopher A. Brown

“Engineers Shall Hold Paramount the Health, Safety, and Welfare of the Public”

Acknowledgments

The team would like to thank the following people for helping us complete this project:

Professor Brown

Professor Hall

Peter Hefti

Toby Bergstrom

Liam Shanahan

Shane Bell

Connor McGuirk

Jeroen Houwen

Thiago Tose

And the Washburn Shops Lab Monitors

Abstract

The goal of this Major Qualifying Project (MQP) was to design and build a ski binding tester that could be built at other locations. The tester was designed to meet the standards described in the American Society for Testing and Materials (ASTM) F504 document. Furthermore, the project aimed to add additional measurements for ski binding performance by analyzing the relationship between linear boot displacement in a ski binding and the moment about the z axis described in ASTM F504. The methods used in this project included the use of the program LabVIEW for data validation purposes, lever arm length ratios for displacement measurements, and two distinct pulley systems that produced forces capable of achieving the ASTM standards. The conclusion drawn from this project was that this ski binding tester, with a few modifications, could be built to produce repeatable test results.

Table of Contents

List of Figures

List of Tables

Definitions

DIN DIN stands for the Deutches Institut für Normung (German Institute for Standardization). This Institute sets standards for many different products, including ski-bindings. In industry, ski bindings are designed to have screws that lock the ski boot in place using a spring mechanism. The more a skier tightens a screw, the more the spring compresses, resulting in a tighter fit around the skier's boot. Therefore, the tighter the screw, the higher the DIN setting.

Mx Moment about x-axis

My Moment about y-axis

Mz Moment about z-axis

Axis Orientations:

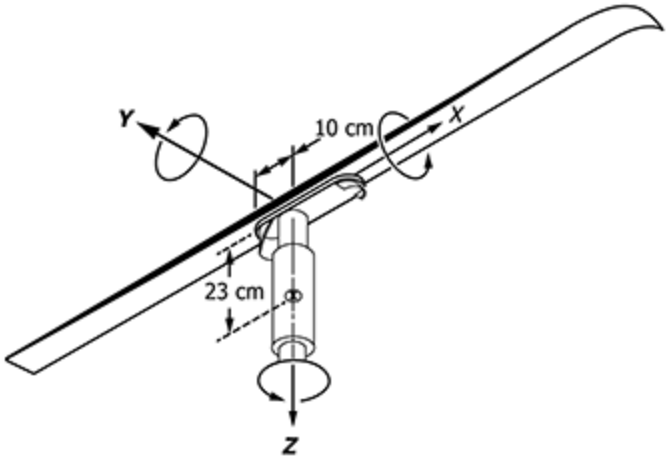

Figure 1: Origin Location and Orientation (ASTM F504 2012)

1. Introduction

1.0. Overreaching Objective

The overreaching objective for this Major Qualifying Project (MQP) was to design and build a ski binding tester that could apply forces at various locations to a mounted ski and induce moments on the ski binding. Another component of the overreaching objective was to provide the capability to assess additional metrics for ski binding performance. At the same time, the tester was designed with cost as a key driver for material selection so the tester could be replicated by others using common materials.

1.1. Objectives

1.1.1. This MQP's first objective was to design and build a ski binding tester that would have repeatable test results comparable to the American Society for Testing and Materials (ASTM) F504 standard. In order to measure success in approaching this objective, our team chose to look at the repeatability of testing results. The repeatability of the results produced by the tester will allow people to set precise DIN settings based on a skier's height, weight, and skill level.

1.1.2. Our second objective was to analyze if there is a relationship between linear boot displacement and M_z that could be used as a measure of binding performance. In addition, this measurement was intended to be taken in a method that has not been done previously. This new method would track displacement of both the heel and toe of a ski binding. This ability is one that would be useful when testing newer skis with alternate, non-standard binding configurations and capabilities.

1.1.3. The third objective was to have the tester measure positive and negative M_x, M_y, and M_z without using sensory equipment on the shaft ("tibia"). We hoped to accomplish this objective in order to prove that simple measuring devices could replace expensive, complicated systems that are currently used and defined in standards.

1.2. State of the Art

1.2.1. To validate the testing capabilities of our tester we wanted to analyze the repeatability of the measurements produced. The term repeatability is defined by the Guide to the expression of uncertainty and measurement (GUM 2008) below in Figure 2. In section 6.6.4 of the ASTM F504 standard it states, "*Repeatability*—Repeated

readings under standard test conditions shall be repeatable to ±1.5 % for moment readings above 50 Nm. Repeatability shall be to ±0.75 % Nm for lower readings" (ASTM F504 2012). Therefore, the measurements in our testing rig will need to match, if not exceed, the repeatability standard.

B.2.15
repeatability (of results of measurements)
closeness of the agreement between the results of successive measurements of the same measurand carried out under the same conditions of measurement

NOTE 1 These conditions are called **repeatability conditions**.

NOTE 2 Repeatability conditions include:

— the same measurement procedure
— the same observer
— the same measuring instrument, used under the same conditions
— the same location
— repetition over a short period of time.

NOTE 3 Repeatability may be expressed quantitatively in terms of the dispersion characteristics of the results.

Figure 2: "Repeatability" (GUM 2008)

1.2.2. A properly engineered ski binding will not only prevent inadvertent release and release under potentially injurious loads, but it will also limit the ski boot's displacement relative to the ski binding, which will allow the skier to steer the skis. Per Ettlinger, "high-performance bindings allow very little movement between the boot and the ski until about 50 to 75 percent of the release setting has been reached." Furthermore, "we can think of this phase of the release-retention cycle as the *control phase"* (Ettlinger 1977). We could not find any current testing using the linear displacement profile as a measurement of binding performance.

One type of technology that enhances binding performance related to boot displacement within the ski binding is a ski binding plate. A component of this ski binding plate, referenced in patent no. US 9,339,719, is the "heel absorption mechanism" that will take in the lateral forces at the heel. In doing so, the absorption mechanism will allow a larger work to release threshold, seen in Figure 3 (Brown et al. 2014). The figure shows loads plotted against displacement within a ski binding. Also in this figure is the adjustment window, which is the area under the graph to which people can vary the settings on their skis. The critical point at the top end of the shape is the point at which the ski falls off. In this configuration, the release point is just below the injury threshold, an ideal configuration for maximum ski performance. This relates to this project because is it a prior example of measured displacement while laterally testing loads on a ski. Our project looked to expand the displacement tracking techniques of systems like the one used to generate the figure.

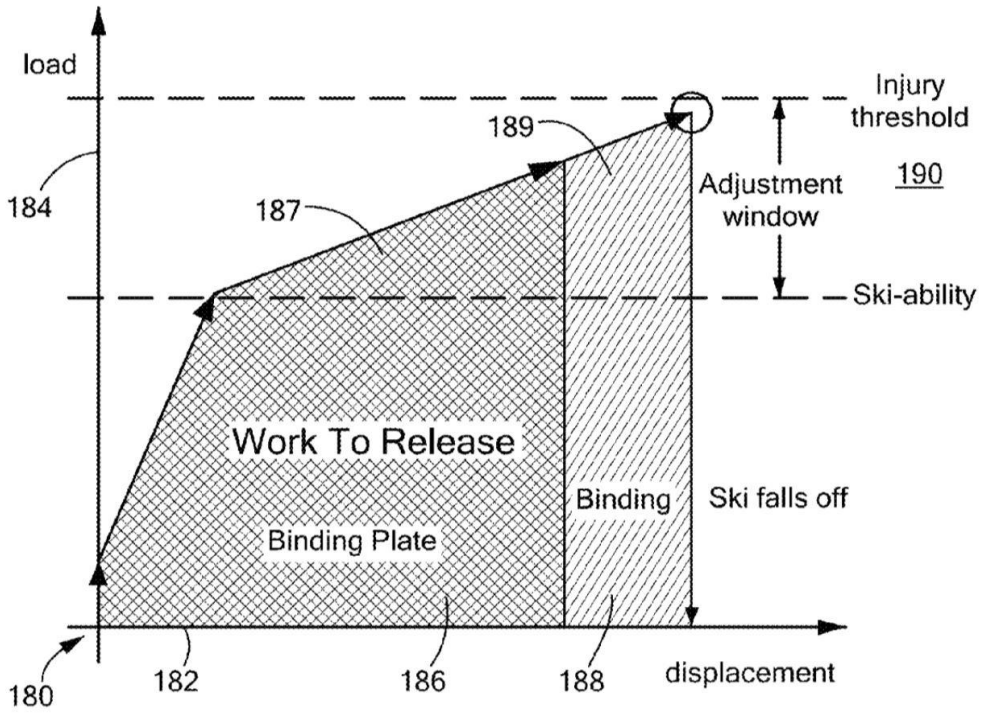

Figure 3: Graph of Load vs. Displacement (Brown et al.)

1.2.3. Early work done regarding testing ski bindings was the Lipe tester (Figure 4), which provided a means for adjusting a binding's retention setting. The tester, patented in 1966, aimed to allow skiers to adjust their own bindings, yet was not precise. The Lipe tester uses a plunger mechanism that applies for to the toe of the ski boot using a compression spring (Lipe et al. 1966). Another ski binding tester invented in 1970, patented in 1972 (Figure 5), by Gloria and Richard Clifford allowed skiers to test the retention of their bindings, while they were mounted on the ski. This tester was much like the Lipe tester however, it accounted for the friction force applied to the ski from the weight of the skier (Clifford et al. 1972).

As ski binding technology improved, so did the testers for said bindings. Some of the modern binding tester include the JETBOND and Safetronic testers. These testers assess the DIN setting using information such as the skier's height, weight, age, and skill level. The JETBOND M, made by Montana, is a tester that tests the torque measurements for the front jaws (Mz) of ski bindings with a load cell. This load cell is connected to an adjustable metal link that fits inside the ski boot, and a motor is used to rotate the metal link in the boot to generate the necessary moment to release. The data is registered for both the inner and outer jaws on a digital interface. The vertical heel release moment (My) is also measured on the same interface using

a different load cell located under the heel of the ski binding. The Safetronic tester, made by Wintersteiger, uses its own custom digital interface, yet tests for the same torque and vertical heel release measurements using a similar procedure as the JETBOND testers.

1.3. Approach

1.3.1. Our testing approach for repeatability was to conduct repetitive trials and analyze the results. The trials were performed using the computer program LabVIEW, which would output the data into spreadsheets. Once the data was collected, statistical analysis was used to find percent deviation.

1.3.2. To accurately measure the linear boot displacement in the ski binding our team used laser measuring tapes to implement a displacement measuring system.

1.3.3. Our approach differed from previous systems because we attempted to measure positive and negative moments using simpler hardware. This change in hardware is being tested to support its validity.

2. Methods

2.1. The method used to design and build the ski binding tester included analyzing what the tester needed to accomplish and then focusing on how to accomplish those things in the least expensive manner. The original design for the tester consisted of a wooden triangular base with a shaft holder at one end of the triangle. The other two ends of the triangle had a metal bar that was positioned to be parallel to the mounted ski. The original pulling system used to apply lateral forces on the ski was a pulley system that attached to the ski at different points. Someone would then manually pull on a rope attached to the pulley resulting in forces being applied to the ski. We noticed that this system was not ideal for the quality of results that we wanted to obtain. In order to address this, we then implemented a winch into the system to decrease human error issues that may have arose with manually pulling through the original pulley system. Once the winch was installed, we noticed that the entire system was bending inwards towards itself. To resolve this issue, we reinforced the base of the system using wooden beams that were placed diagonally to support the moments incurred by the system.

To measure our success of our design, we chose to look at the repeatability of the system compared to the F504 standard for repeatability. We took 12 different trials of the same test, and looked at the variation in the results from each set of the 10 Vishay strain gauges (Figure 4) that capture data in our system. These strain

gauges function by using the displacement of the grid (shown below) to act as a variable resistor.

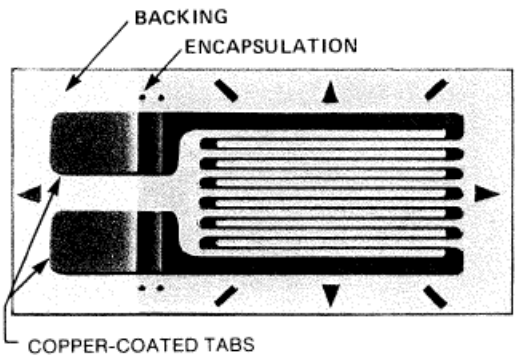

Figure 4: VISHAY Strain Gauge from ES3901 lab report

We chose to layout our strain gauges in a half bridge design to measure compression on one side of our shaft and tension on the other side. These two resistors worked together to accurately measure the bending moment in the shaft. A diagram of a half-bridge is shown below in Figure 5. In this configuration, two strain gauges, one in tension and one in compression, are used together with two known resistors to measure a bending moment on an object.

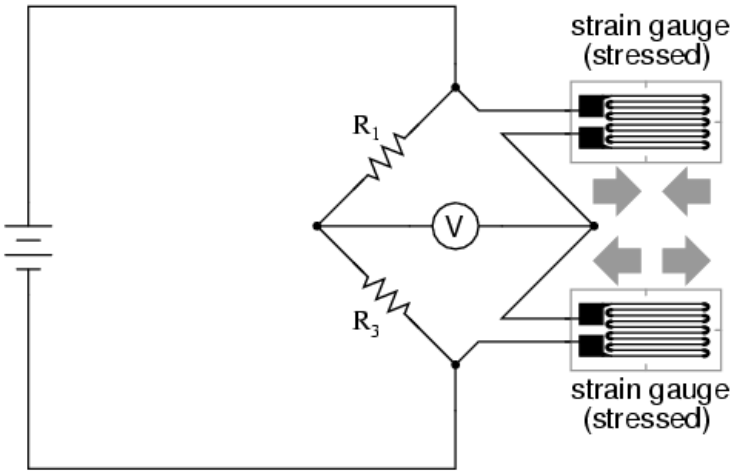

Figure 5: Diagram of Half Bridge from google images

2.2. In order to assess the relationship between linear displacement and moment, we planned to plot linear displacement against M_z for five data trials for each of three different skis. We attempted to measure the displacement using two laser tape measures that we bought from Amazon.com. One of these devices was aimed near the tip of the ski while the other was aimed near the tail of the ski.

To compile all the data into one document we used inexpensive computer webcams. These cameras captured live results from the devices and combined all the results on one platform called ManyCam. One camera was mounted to each of the laser tapes and scales. The use of these cameras contributed to the modularity of the system because they allowed for many different devices to be utilized at different locations and still compile the data in real time.

The strategy used measuring linear displacement involves an amplification of the boot displacement within the binding. By using the length of the ski, we could calculate the boot displacement within the binding by observing movement of the ends of the ski. We set up laser measuring tapes at the tip and rear of the ski to measure ski displacement when there was a lateral force applied to it, and then used the relationship demonstrated by Figure 6 to calculate boot displacement within the binding.

- $\mathbf{D_O}$ is the output distance that the load force is moved
- $\mathbf{D_I}$ is the input distance that the effort forces moves
- $\mathbf{d_O}$ is the length of the load or output arm
- $\mathbf{d_I}$ is the length of the effort or input arm

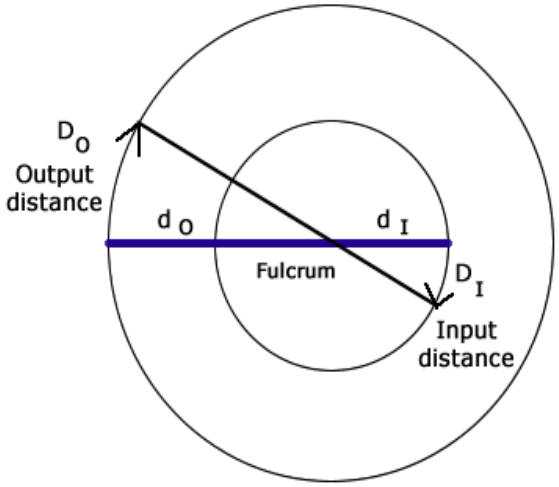

Distance relationship to lever arms with Class 1 lever

$\theta = \mathbf{D_O}/\mathbf{d_O} = \mathbf{D_I}/\mathbf{d_I}$, you get the equation:

$$\mathbf{D_O}/\mathbf{D_I} = \mathbf{d_O}/\mathbf{d_I}$$

Figure 6: Description for the relationship of the measured linear displacements

2.3. To determine if the fish scale was a viable replacement for the instrumented shaft, we compiled data in excel from LabVIEW. Our LabVIEW program took data from the strain gauges and the fish scale, which read the force from the winch in the x direction. We used the webcams to easily read the data from the fish scales, see

Figure 7. These cameras were mounted directly to the scales with metal brackets that were made by bending steel plates and fastening them to the shackles in the scales. The images are provided to assist in recreation of these systems. Six trials were performed over five different positions on the ski. These points were chosen based on the F504 standard with an additional point in an area of special interest. The special area was under the boot and one of the test points within the binding is one that is not stated in the current F504 standard.

Figure 7: Images of Load Scale with Camera Setup

In excel we graphed resistance data outputted from the strain gauges versus the fish scale data. The trend line of the graph would tell how accurate the fish scale reading was. This was also repeated with a preload ($+M_Y$) applied to the ski. The preload was applied through a pneumatic system that consisted of a pair of pneumatic cylinders. These cylinders pushed on a bracket attached to a cord that pulled down on the ski. We chose a preload force of 230 Newtons and applied it 350 mm away from the test shaft. This distance was taken from the F504 standard. To read the applied preload force we had another fish scale in the preload line. Figure 8 is below to aid in the recreation of this system. When viewing this data, another graph was added to compare data produced from the strain gauges placed in the y axis orientation at 33 cm to the force of the fish scale. The trend line of this data was used to see how accurate the fish scale was.

Figure 8: Images of Preloading System as Built

3. Testing Procedure

3.1. To test repeatability, we applied known forces in the x axis, y axis, and z axis orientations of the boot. We used approximately 6 different forces per trial and used these to generate lines that plotted force against measured resistance. Applied forces were measured using a "fish scale"while resulting moments where measured using the strain gauges shown in Figure 4. The slopes and intercepts of these generated lines were then analyzed for variation across the trials. The data was also used to calibrate the strain gauges to have them read out in moments instead of resistance.

In order to perform a trial in the x direction, we placed the instrumented shaft on the rig with the toe of the boot pointing in the along the x direction. Then two c clamps need to be added in order to form an anchor point on to which we could pull for our tests (Figure 9). Now start the LabVIEW program and collect the first point with no equipment hanging on the boot. This is the zero point. Next attach the fish scale attached to the winch and let it hang. Take the reading from the fish scale and record it. Now retract the winch and collect the point that the fish scale reads. Do this 3-4 more times to get enough data. Then hit end program to stop the test.

Figure 9: Image of Clamping Technique

To do a trial in the y direction it is almost the same as the x direction. But when doing y test, we turned the boot on the rig so that the toe of the boot pointed in the positive y direction. There was also a different method of clamps to hook the fish scale to the boot. We used a u bolt to hook around the boot and the back of the shaft then attached the fish scale with a carabineer to the bolt. Now the same procedure is followed that was done for the test in the x direction.

In order to perform a test in for the moment in the z direction we used a torque measuring device that we put between the instrumented shaft and the testing rig. Next, we attached a 2x4 on top of the boot with c clamps. This was done so that we could twist the boot and hold it by hand in a controlled form. Like the other test, we collected a point when there was zero torque applied. Then using 2 people they would twist the 2x4 until a desired torque was read and a third person would record the point into lab view. Points we tried to get points close to 30 Nm, 60 Nm, 90 Nm, 120 Nm, 150 Nm, and 180 Nm.

3.2. To test for the linear displacement of the ski when pulling, we set up two laser mearing devices on the back frame. One of these devices was near the tip of the ski while the other was near the tail. The sensors were set up to measure the distance from their positions to the near edge of the ski. To simplify this process, we applied paper flags to the edge of the ski to give the lasers larger targets to track. We used a camera system, coupled with the software ManyCam, to relay the data to one central laptop in real time. We used this system to monitor the positions of the tip and tail while various forces were applied. These measurements were then converted into

movement at the toe using the formula from Figure 6. This data was then all recorded in excel. Using excel, we looked at the relationships from one point to another.

3.3. We started one of these tests with the ski on the rig with no force applied. Then the clamping device needed to be placed on the ski in a location based on a measurement described in the F504 standard. For points outside of the binding, we used a Velcro moving strap with a carabineer that attached the fish scale to the winch. To make sure the strap didn't move, a c clamp was used in addition to the strap. For a point located within the binding, only a c clamp was used and a carabineer pulled on the handle of the clamp. This was done because the moving straps could not be attached at this location. The next steps included starting the LabVIEW program, entering a zero point, and recording that point for 3 seconds. Next, the fish scale was attached with the cable from the winch to the clamp. We then read the point from the fish scale, wrote in the value for force, and held the button to record it for a few seconds. After, we pulled in the winch and collected a few more data points. The data was then exported to the data out excel file where it could be opened and saved as the respective test and trial number.

When a preload was added, a Velcro moving strap was used as a clamp at a specified point on the F504. Then, a zero point was taken following the same procedure mentioned in above. Next, two cables, one from the winch and one from the pneumatic system, were attached to the preload clamp. We turned on the air compressor and added enough pressure to pull on the ski until the desired preload force was reached. Following the same procedure as before, we took down the point that the fish scale read, while making sure to record the data for 3 seconds. See Figure 10 below. The figure shows the wooden tester constructed and in place with a ski mounted on it. In addition to the structural frame, in the image one can also see the two safety guards mounted around the ski in order to prevent the ski from

leaving the device upon the sudden release of energy that is associated with binding release.

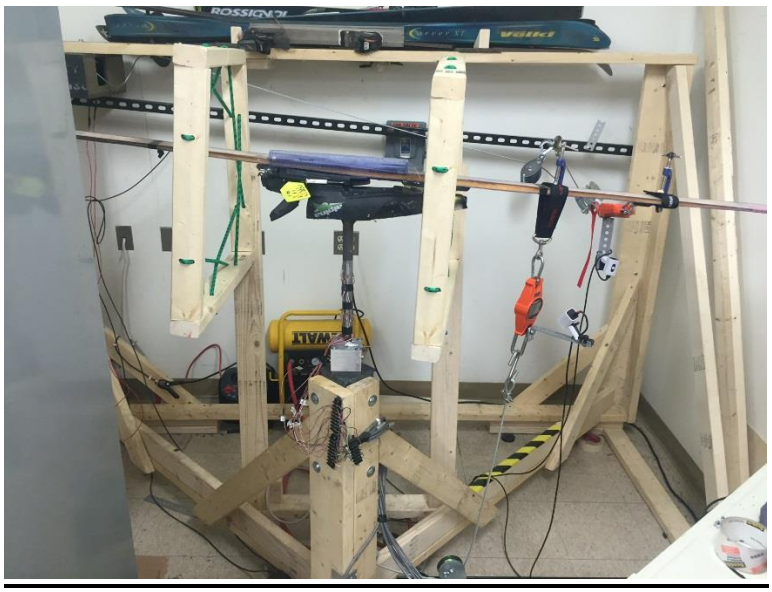

Figure 10: Image of Tester in Place

4. Results

4.1. From the data acquired, percent deviations were calculated for each set of strain gauges. The resulting percent deviations can be seen in Table 2. The data in the table was generated by dividing the average deviation of trials for a set by the average values of the trials. The data across the trials all appeared to be within 2% across the trials. The highest value, moment about the x axis at 23 cm from the sole of the boot, was likely due to faulty equipment. This error is described in better detail in Section 5.1.

Table 4, located in appendix I, displays the calculated slopes, intercepts, and r-squared values for the data that we took. In addition, an example of raw data and the resulting graph used is shown in Table 3 in appendix I. We used the data in Table 4 to calculate the data in Table 1. Table 1, below, shows the calculated data used to draw conclusions.

	Average		Average Deviation		
	Slope	Intercept	Slope	Intercept	Percent Deviation
X	-15772.17	-9.80	286.72	8.18	-1.82%
	-10393.51	-7.82	172.83	6.36	-1.66%
Y	-14870.75	17.22	116.04	7.01	-0.78%
	-10388.58	-4.09	109.24	1.94	-1.05%
Z	10790.03	0.74	168.27	2.05	1.56%

Table 1: Values Used To Calculate Percent Deviation

Table 2, also below, shows the final values of percent deviations that we used to assess our success in completing our objective. The data presented is the percent deviation of the slope values calculated in Table 4.

	Percent Deviation		
	Moment about x-axis	Moment about y-axis	Moment about z-axis
230 ± 5 mm	1.82%	0.78%	1.56%
330 ± 5 mm	1.66%	1.05%	

Table 2: Percent Deviation of Moments Across 12 Trials in Each Orientation.

4.2. Based on the captured data, our team was not able to generate viable results for angular boot displacement due to the inaccuracy of the laser measuring tapes used. This is largely caused by the inability of our laser setup to capture accurate or precise data. The acquired data did not show any viable relationships and could not be used. Because of this we were unable to develop an assessment regarding the validity of the relationship.

4.3. The data outputted by LabVIEW was placed in an excel spreadsheet where it had electrical values that were measured by the strain gauges and adjusted data that converted the electrical signals to forces and moments. The data we were most interested in was from the M_x at 33 cm, M_y at 33 cm, and the M_z strain gauges. The M_x at 33 cm and the M_y at 33 cm gauges' adjusted output was the forces that pulled along their axes and the z gauge read M_z. These numbers were graphed in the y axis versus the data that the fish scale on the winch read. A trend line was formed and the slope, intercept and r-squared values were generated and then put on our own excel sheet where we took the average and percent deviation between the different

trials and spots on the ski. The averages of the trials, percent deviation and error at different positions are shown in TABLES 5-9 in Appendix I.

When a preload was added, the method of analyzing the data stayed the same, but a row was added to analyze the relationship between the reading of the y strain gauge and the reading of the fish scale attached to the preload. The averages of the trials and the percent deviation and error at different positions with the added preload are shown in TABLES 10-14 In Appendix I.

5. Discussion

5.1. From the data gathered, we found that all the testing rig data was repeatable to within ± 2%. As stated above, the F504 standard calls for repeatability to be within ± 1.5%. We believe that this would be attainable after modifications to the tester that would take some variance out of the data.

After the completion of the testing for this objective, we developed a problem with the amplifier that was used to capture the data from the strain gauges measuring M_x at 23 cm. The amplifier stopped functioning properly and would not produce consistent data. After this occurred, we revised our data and found that the samples gathered from the strain gauges measuring M_x at 23 cm had more noise than samples gathered by the strain gauges measuring M_x at 33 cm, and therefore generated worse data. This could be one possible explanation for why the data from this position had the highest error of all the other positions. We were also having similar problems in our amp for M_y at 23 cm. Moving forward we were not able to use these amps to produce data.

5.2. Our second objective was to find a relationship between the linear boot displacement within the ski binding and the moment applied in the z axis to assess this as a possible parameter for measuring binding performance. Unfortunately, the equipment used to implement the measuring system mentioned in the methods section was not accurate enough. The laser tapes were accurate to ±1/8 of an inch (0.3175 cm), which was theoretically able to calculate the displacement at toe and heel of the boot. However, the issue that arose was that the measuring tapes simply did not measure the accurate displacement at the edge of the ski.

5.3. Ideally, when looking at the slopes generated for the M_x line, we would want it to equal one. The y values are looking at the force that the strain gauges read in the x

direction and the x values are looking at the force that the fish scale is reading from the pull of the winch. Taking the slope of this data should result in a value of one. After taking the average of the slopes and the average deviation, we calculated the percent deviation and percent error based on those numbers.

Following the same logic as objective 1, If our percent deviation was within ±1.5% we could conclude that the data was repeatable. If our percent error was within ±2%, what we found in objective 1, we could have considered our data to be accurate enough where we would be able to switch out the strain gauges for less expensive fish scales. In the trials without preload, our values of percent error did not fall within the range of 2%. However, our numbers for percent deviation were very low and did fall within the range of ±1.5%. This being said, there was one exception, at the zero spot the percent deviation was at 2.85%.

When looking at the generated line for M_y, ideally the slope should be 0 and the intercept should be zero. This should be the case considering there was no preload and the only force is in the x direction. Yet, our data shows that there is some force in the y direction. This could have been caused by the measuring equipment that was hanging off the ski. It should be noted that without the strain gauges there would be no way of measuring this small amount of weight. When analyzing this data, the values for average r-squared, percent deviation and percent error were not seen as useful data points.

Finally, when looking at the M_z line the slope should equal the distance where the pull on the ski took place. The y data produced by the strain gauges reads M_z and the data on the x axis is the force in the x direction. If our percent deviation was within ±1.5% we could conclude that the data was repeatable. If our percent error was within ±2% we could have considered our data to be accurate enough where we would be able to switch out the strain gauges for less expensive fish scales.

The percent error of the z gauge was much greater than what we wanted, but the percent deviation was still within the range of ±1.5%. There is one exception to this and it is at the zero point again. Since our data was shown to be precise but not accurate the error could be something that came from calibration of the amps used to collect the data.

When we did this test with the added preload it off balanced the data by a great amount. This could be caused by our preload system being hooked up to a fixed point along a rail. The point couldn't move in the x axis with the ski being pulled and ended up adding unwanted force on the x axis that couldn’t be accounted for by the fish scales.

Looking back at the data we do not have accurate enough values to say that we can replace the strain gauges with the fish scales. However we do believe that with some modifications to the preload system and more testing you could eventually replace the strain gauges.

6. Suggestions for improvement

6.1. The first improvement that we would suggest to simplify the process would be to add additional programming into the LabVIEW program for easier calibrations. Currently the calibration data must be analyzed trial by trial manually in Microsoft Excel. With a better understanding of LabVIEW and its programming, these calculations could be built into the software and the testing and analysis could all be done with much less effort. This process would help to simplify the data collection and help record more consistent data

6.2. To conclusively test for the relationship between linear displacement and moments generated in the z axis there needs to be a better way of tracking the angular displacement. We attempted to measure displacement two different ways and neither of them accurately tracked the motion. The focus of improvement for this objective would be to develop a better way of tracking the motion of the ski relative to the boot. This system would need to be able to track both motion on the toe, as well as motion of the heel displacing laterally in the boot as some newer bindings have displacement in both locations.

A second improvement that we would suggest for others continuing research on this topic would be to look at the relationship of angular displacement rather than linear displacement. This is because data would be more comparable across different testers. This is because the linear displacement would be affected by different boot sizes. On the other hand, angular displacement would be a better metric to compare across different skis and testing setups. One thing to keep in mind is that for bindings that displace at the toe and the heel, linear displacement at each would be a better measurement because angular would not be able to account for the additional motion.

6.3. The system we had in place for a preload system was too rigid and affected the force in the x direction too much. If there was a way so the preload force can move with the ski

as its being pulled instead of a fixed point then this would be a viable way of measuring the preload.

References

A brief introduction to standards. (n.d.). Retrieved January 14, 2017, from http://www.din.de/en/about-standards/a-brief-introduction-to-standards

ASTM F504-05 (2012) Standard Test Method for Measuring the Quasi-Static Release Moments of Alpine Ski Bindings, ASTM International, West Conshohocken, PA, 2012, https://doi.org/10.1520/F0504-05R12

ASTM F939-12 (2012) Standard Practice for Selection of Release Torque Values for Alpine Ski Bindings, ASTM International, West Conshohocken, PA, 2012, https://doi.org/10.1520/F0939-12

ASTM F1061-0 8 (2013) Standard Specification for Ski Binding Test Devices, ASTM International, West Conshohocken, PA, 2013, https://doi.org/10.1520/F1061

Brown et al. (2016). U.S. patent No. 9,339,719 B2. Worcester Polytechnic Institute.

Clifford, Gloria L. & Clifford, Richard P. (1972). U.S. Patent No. 3,663,594. Washington, DC: U.S. Patent and Trademark Office.

Ettlinger, C. F., Dodge, D., Johnson, R. J., Shealy, J. E., and Sargent, M. (2010). "Retention Requirements for Alpine Ski Bindings," *Journal of ASTM International*, Vol. 7, No. 6, 2010, pp. 1-22, https://doi.org/10.1520/JAI102978. ISSN 1546-962X

Ettlinger, Carl. (1977). “Bindings and Skiing Performance The Other Side of the Coin.” *Skiing*,Vol. 29, No. 6, Feb. 1977, pp. 86-89.

Fixed Bail Snap Shackles. (n.d.). Retrieved January 14, 2017, from https://www.westmarine.com/buy/ronstan--fixed-bail-snap-shackles--P002_060_001_501?recordNum=25

HAMMERHEAD HLMT100 Compact Laser Measuring Tool - 100 Feet. (n.d.). Retrieved January 14, 2017, from https://www.amazon.com/HAMMERHEAD-HLMT100-Compact-Laser-Measuring/dp/B00N2GXHGI/ref=sr_1_3?s=industrial&ie=UTF8&qid=1484431038&sr=1-3&keywords=laser%2Btape%2Bmeasur

Hopkins, M. D., & D., H. M. (n.d.). Patent US6007086 - Electric ski binding system. Retrieved January 14, 2017, from https://www.google.com/patents/US6007086

Hughes, Ifan;Hase, Thomas. (2010). *Measurements and their Uncertainties*. OUP Oxford, 2010. 3 January 2017 http://www.myilibrary.com?ID=273234

Increasing Distance Moved with a Lever. (n.d.). Retrieved January 14, 2017, from http://www.school-for-champions.com/machines/levers_increase_distance.htm#.WHqb8_krKUk

JCGM 100:2008. Evaluation of measurement data – Guide to the expression of uncertainty in measurement, Joint Committee for Guides in Metrology.

Lipe, Gordan C. & Hinds, Charles W. (1966). U.S. Patent No. 3,289,472. Washington, DC: U.S. Patent and Trademark Office.

Montana (2007). JETBOND ST/SK. Retrieved November 28, 2013, from http://www.montana-international.com/en/products/machines/ski-binding-adjustment/jetbond-st-sk/

Wintersteiger (2011). Speedtronic Pro. Retrieved November 30, 2013, from https://www.wintersteiger.com/en/Ski-Service-and-Rental/Ski-Service-Machines/New-Machines-Ski-and-Snowboard-Service/Binding-Adjustment/238-Safetronic

APPENDIX I: Additional Tables & Figures

Mx 23 data	Inputted Force	Mx 33 data
-0.00035	0	0.000078
-0.00117	0	0.000082
-7.8E-05	0	0.000095
0.000468	0	0.000098
0.000189	0	0.000094
-0.00054	0	0.000125
-0.0002	0	0.000077
-0.00097	0	0.00009
0.00005	0	0.000107
-0.00054	0	0.000083
-0.00029	0	0.00014
0.002909	0	0.00007
-0.0004	0	0.000095
0.000471	0	0.00009
0.00006	0	0.000093
0.000144	0	0.000162
-8.3E-05	0	0.000085
0.001067	0	0.000144
0.000178	0	0.000085
0.000328	0	0.00014
0.000837	0	0.000106
0.000232	0	0.00009
0.000178	0	0.000125
-0.00033	0	0.000073
-0.00023	0	0.000139
-0.002	37.2	-0.00308
-0.00205	37.2	-0.00312
-0.00198	37.2	-0.00312
-0.00202	37.2	-0.00312
-0.00198	37.2	-0.00312
-0.00198	37.2	-0.00309
-0.00203	37.2	-0.00311
-0.00201	37.2	-0.00313
-0.00211	37.2	-0.0031
-0.00204	37.2	-0.00317
-0.00204	37.2	-0.00308
-0.00207	37.2	-0.00309
-0.002	37.2	-0.00308
-0.00213	37.2	-0.00311
-0.00202	37.2	-0.00305
-0.002	37.2	-0.00309
-0.00197	37.2	-0.00312
-0.00195	37.2	-0.0031
-0.00199	37.2	-0.00309
-0.00202	37.2	-0.00309
-0.00199	37.2	-0.00308
-0.00197	37.2	-0.00311
-0.00196	37.2	-0.00309
-0.00192	37.2	-0.00302
-0.00201	37.2	-0.00311
-0.00201	37.2	-0.00312
-0.002	37.2	-0.0031
-0.00225	37.2	-0.0031
-0.002	37.2	-0.00311
-0.00202	37.2	-0.00308
-0.00199	37.2	-0.0031
-0.0019	37.2	-0.00308
-0.002	37.2	-0.00309
-0.00201	37.2	-0.00308
-0.00207	37.2	-0.0031
-0.00207	37.2	-0.00311
-0.00202	37.2	-0.0031
-0.00193	37.2	-0.00313
-0.00198	37.2	-0.00315
-0.00203	37.2	-0.0031
-0.00202	37.2	-0.00309
-0.00204	37.2	-0.00305
-0.00208	37.2	-0.00308
-0.00198	37.2	-0.00308
-0.00197	37.2	-0.00311
-0.00207	37.2	-0.0031
-0.00199	37.2	-0.00311
-0.00192	37.2	-0.00311
-0.00187	37.2	-0.00312
-0.00198	37.2	-0.0031
-0.00197	37.2	-0.00312
-0.00201	37.2	-0.00314
-0.00187	37.2	-0.0031
-0.00184	37.2	-0.00307
-0.00429	66.6	-0.00613
-0.00402	66.6	-0.00621
-0.00417	66.6	-0.00613
-0.00403	66.6	-0.00615
-0.00401	66.6	-0.00616
-0.00407	66.6	-0.00615
-0.00397	66.6	-0.00614
-0.0039	66.6	-0.00614
-0.00401	66.6	-0.00613
-0.00401	66.6	-0.00615
-0.00405	66.6	-0.00613
-0.00402	66.6	-0.00614
-0.00405	66.6	-0.00616
-0.00398	66.6	-0.0061
-0.00412	66.6	-0.00619
-0.00401	66.6	-0.00614
-0.00414	66.6	-0.00615
-0.00404	66.6	-0.00616
-0.0044	66.6	-0.00617
-0.00405	66.6	-0.00615
-0.00402	66.6	-0.00617
-0.00405	66.6	-0.00618
-0.00392	66.6	-0.0062
-0.00404	66.6	-0.00616
-0.00402	66.6	-0.00615
-0.00401	66.6	-0.00617
-0.00414	66.6	-0.00616
-0.00401	66.6	-0.00615
-0.00395	66.6	-0.00615
-0.00396	66.6	-0.00616
-0.004	66.6	-0.00612
-0.00401	66.6	-0.00613
-0.00404	66.6	-0.00616
-0.00407	66.6	-0.00615
-0.00401	66.6	-0.00616
-0.00402	66.6	-0.00616
-0.00399	66.6	-0.00613
-0.00404	66.6	-0.00615
-0.004	66.6	-0.00613
-0.004	66.6	-0.00615
-0.00395	66.6	-0.00611
-0.00955	142.1	-0.01456
-0.00953	142.1	-0.0145
-0.0095	142.1	-0.01454
-0.00959	142.1	-0.01449
-0.00953	142.1	-0.01446
-0.00955	142.1	-0.01444
-0.00958	142.1	-0.01449
-0.00942	142.1	-0.01447
-0.00947	142.1	-0.01446
-0.00952	142.1	-0.01442
-0.00955	142.1	-0.01444
-0.00959	142.1	-0.01445
-0.00947	142.1	-0.01445
-0.00948	142.1	-0.01447
-0.00949	142.1	-0.01447
-0.00963	142.1	-0.01447
-0.00952	142.1	-0.01447
-0.0095	142.1	-0.01446
-0.00946	142.1	-0.01445
-0.0095	142.1	-0.01439
-0.00951	142.1	-0.01439
-0.00943	142.1	-0.01442
-0.00946	142.1	-0.01446
-0.00949	142.1	-0.01439
-0.00949	142.1	-0.01442
-0.00944	142.1	-0.01441
-0.0097	142.1	-0.01438
-0.00945	142.1	-0.01445
-0.00952	142.1	-0.01443
-0.00946	142.1	-0.01438
-0.00955	142.1	-0.01443
-0.00947	142.1	-0.01441
-0.00956	142.1	-0.0144
-0.00951	142.1	-0.0144
-0.00949	142.1	-0.01439
-0.00946	142.1	-0.01443
-0.00952	142.1	-0.01443
-0.0095	142.1	-0.01439
-0.00951	142.1	-0.01441
-0.00965	142.1	-0.0144
-0.00948	142.1	-0.0144
-0.0095	142.1	-0.01443
-0.00931	142.1	-0.01433
-0.00949	142.1	-0.01439
-0.00943	142.1	-0.01441
-0.00945	142.1	-0.01445

-0.00943	142.1	-0.01441
-0.02404	380.2	-0.03664
-0.02413	380.2	-0.03661
-0.02403	380.2	-0.03657
-0.02427	380.2	-0.03661
-0.02404	380.2	-0.0366
-0.02402	380.2	-0.0366
-0.02405	380.2	-0.03657
-0.02422	380.2	-0.03663
-0.02405	380.2	-0.03659
-0.02401	380.2	-0.03658
-0.02381	380.2	-0.03659
-0.02399	380.2	-0.0366
-0.02404	380.2	-0.03658
-0.02411	380.2	-0.03658
-0.02397	380.2	-0.03656
-0.02403	380.2	-0.03655
-0.02396	380.2	-0.03653
-0.02399	380.2	-0.03654
-0.02391	380.2	-0.03653
-0.02387	380.2	-0.03652
-0.02398	380.2	-0.03655
-0.024	380.2	-0.03653
-0.02408	380.2	-0.03655
-0.02399	380.2	-0.03653
-0.02398	380.2	-0.03653
-0.02396	380.2	-0.03653
-0.02394	380.2	-0.03652
-0.02396	380.2	-0.03652
-0.02397	380.2	-0.0365
-0.02393	380.2	-0.0365
-0.02398	380.2	-0.03653
-0.02399	380.2	-0.0365
-0.02397	380.2	-0.03648
-0.02398	380.2	-0.03648
-0.02398	380.2	-0.03648
-0.02394	380.2	-0.03648
-0.02395	380.2	-0.03647
-0.02396	380.2	-0.03646
-0.02408	380.2	-0.03647
-0.01152	173.5	-0.01755
-0.01154	173.5	-0.01755
-0.01146	173.5	-0.01755
-0.01155	173.5	-0.01754
-0.01151	173.5	-0.01758
-0.01154	173.5	-0.01755
-0.0115	173.5	-0.01755
-0.01149	173.5	-0.01761
-0.01152	173.5	-0.01758
-0.01153	173.5	-0.01755
-0.01149	173.5	-0.01757
-0.01154	173.5	-0.01758
-0.01152	173.5	-0.01757
-0.0115	173.5	-0.01756
-0.01152	173.5	-0.01756
-0.01149	173.5	-0.01754

-0.01155	173.5	-0.01757
-0.01152	173.5	-0.01755
-0.01153	173.5	-0.01757
-0.01152	173.5	-0.01755
-0.01152	173.5	-0.01757
-0.01156	173.5	-0.01754
-0.01143	173.5	-0.01761
-0.01683	259.7	-0.02564
-0.01683	259.7	-0.02556
-0.01684	259.7	-0.02563
-0.01683	259.7	-0.02566
-0.01683	259.7	-0.02566
-0.01685	259.7	-0.02565
-0.01681	259.7	-0.02564
-0.01717	259.7	-0.02566
-0.01685	259.7	-0.02565
-0.01684	259.7	-0.02565
-0.01684	259.7	-0.02565
-0.01682	259.7	-0.02558
-0.01681	259.7	-0.02566
-0.01682	259.7	-0.02562
-0.01678	259.7	-0.02567
-0.01684	259.7	-0.02564
-0.01684	259.7	-0.0256
-0.0168	259.7	-0.02565
-0.01679	259.7	-0.02563
-0.01684	259.7	-0.02567
-0.01682	259.7	-0.02564
-0.01682	259.7	-0.02565
-0.01683	259.7	-0.02566
-0.01684	259.7	-0.02565
-0.01684	259.7	-0.02563
-0.01683	259.7	-0.02558
-0.01684	259.7	-0.02565
-0.01686	259.7	-0.02565
-0.01685	259.7	-0.02563
-0.01681	259.7	-0.02561
-0.01684	259.7	-0.02567
-0.01679	259.7	-0.02569
-0.01682	259.7	-0.02563
-0.01695	259.7	-0.02564
-0.01682	259.7	-0.02563
-0.01683	259.7	-0.02562
-0.01684	259.7	-0.02564
-0.01658	259.7	-0.02563
-0.01683	259.7	-0.02564
-0.01681	259.7	-0.02568
-0.01692	259.7	-0.02569
-0.01675	259.7	-0.02563
-0.01684	259.7	-0.02569
-0.01685	259.7	-0.02563
-0.01682	259.7	-0.02553
-0.01683	259.7	-0.02565
-0.01684	259.7	-0.02566
-0.02063	324.4	-0.03154
-0.02072	324.4	-0.03149

-0.02061	324.4	-0.03149
-0.02067	324.4	-0.03146
-0.02064	324.4	-0.03145
-0.02066	324.4	-0.03151
-0.0206	324.4	-0.03149
-0.02067	324.4	-0.03151
-0.02068	324.4	-0.03147
-0.02064	324.4	-0.0315
-0.02064	324.4	-0.03135
-0.02065	324.4	-0.03149
-0.02069	324.4	-0.03147
-0.02067	324.4	-0.03148
-0.02066	324.4	-0.03149
-0.02067	324.4	-0.03149
-0.02061	324.4	-0.0315
-0.02064	324.4	-0.03147
-0.02064	324.4	-0.0315
-0.02064	324.4	-0.03149
-0.02066	324.4	-0.03147
-0.02063	324.4	-0.03148
-0.02043	324.4	-0.03146
-0.02067	324.4	-0.03148
-0.02071	324.4	-0.03146
-0.02069	324.4	-0.03146
-0.02066	324.4	-0.03147
-0.02056	324.4	-0.03149
-0.02068	324.4	-0.03147
-0.02066	324.4	-0.03155
-0.02065	324.4	-0.03151
-0.02062	324.4	-0.03147
-0.02064	324.4	-0.03146
-0.0207	324.4	-0.03147
-0.02064	324.4	-0.0315
-0.02067	324.4	-0.03146
-0.02052	324.4	-0.03149
-0.02064	324.4	-0.03145
-0.02079	324.4	-0.03151
-0.02068	324.4	-0.03148
-0.02065	324.4	-0.03149
-0.02067	324.4	-0.03148
-0.02063	324.4	-0.03148
-0.0206	324.4	-0.03149
-0.02067	324.4	-0.03147
-0.02065	324.4	-0.03152
-0.02071	324.4	-0.0315
-0.02074	324.4	-0.03148
-0.0206	324.4	-0.03148
-0.02063	324.4	-0.03148
-0.02064	324.4	-0.03145
-0.02066	324.4	-0.03149
-0.02064	324.4	-0.03147
-0.02065	324.4	-0.03151
-0.02077	324.4	-0.03148
-0.02065	324.4	-0.03149
-0.02062	324.4	-0.03148
-0.02063	324.4	-0.03148

Table 3: Raw Data Example from Objective 1

Test	Gauge set	Calculated Slope	Calculated Intercept	R^2
x1 12/7	x23	-15968	-9.7843	0.9999
x1 12/7	x33	-10346	-0.6339	1
x2 12/7	x23	-15805	-17.877	0.9988
x2 12/7	x33	-10265	-8.6858	0.9973
x3 12/7	x23	-16171	-23.779	0.9997
x3 12/7	x33	-10574	-15.692	1
x4 12/7	**x23**	**-15560**	**1.3456**	**0.9981**
x4 12/7	**x33**	**-10228**	**1.0439**	**0.9988**
x5 12/8	x23	-16865	-36.804	0.939
x5 12/8	x33	-11107	-37.264	0.9429
x6 12/8	x23	-14982	-5.0018	0.9984
x6 12/8	x33	-9958.1	-5.4428	0.9996
x7 12/8	x23	-15751	-1.7872	0.9992
x7 12/8	x33	-10486	-2.2357	0.9999
x8 12/12	x23	-15461	-1.2493	0.9997
x8 12/12	x33	-10215	-1.2506	0.9998
x9 12/12	x23	-15649	-4.951	0.9992
x9 12/12	x33	-10343	-5.1628	0.9996
x10 12/12	x23	-15770	-6.1541	0.9981
x10 12/12	x33	-10444	-6.3303	0.9996
x11 12/12	x23	-15642	-5.0131	0.9982
x11 12/12	x33	-10391	-5.7999	0.9997
x12 12/12	x23	-15642	-6.5572	0.9991
x12 12/12	x33	-10365	-6.377	0.9998
y1 12/12	y23	-15436	-3.742	0.9996
y1 12/12	y33	-10330	0.5369	0.9998
y2 12/12	y23	-14916	11.174	0.9994
y2 12/12	y33	-10385	-2.1498	0.9996
y3 12/13	y23	-14916	11.174	0.9994
y3 12/13	y33	-10385	-2.1498	0.9996
y4 12/13	y23	-14905	14.391	0.9995
y4 12/13	y33	-10339	-2.5744	0.9998
y5 12/13	y23	-14862	14.369	0.9995
y5 12/13	y33	-11044	-11.705	0.9922
y6 12/13	y23	-14682	15.276	0.9993
y6 12/13	y33	-10256	-4.6951	0.9996
y7 12/13	y23	-14877	15.86	0.9995
y7 12/13	y33	-10370	-4.3165	0.9997
y8 12/13	y23	-14821	21.48	0.9992
y8 12/13	y33	-10329	-5.7453	0.9994
y9 12/13	y23	-14758	26.738	0.9996
y9 12/13	y33	-10306	-3.5514	0.9998
y10 12/13	y23	-14718	26.198	0.9995
y10 12/13	y33	-10276	-4.313	0.9997
y11 12/13	y23	-14747	28.025	0.9994
y11 12/13	y33	-10302	-3.0585	0.9997
y12 12/13	y23	-14811	25.721	0.9995
y12 12/13	y33	-10341	-5.3961	0.9997
z1 12/13	Z	10714.6	-3.1825	0.9991

z2 12/13	Z	10855.6	2.5348	0.9992
z3 12/13	Z	10820	2.4398	0.9996
z4 12/13	Z	10960.2	2.2021	0.9997
z5 12/13	Z	10745	1.1969	0.9994
z6 12/13	Z	11141	4.5678	0.9989
z7 12/13	Z	10537	3.7886	0.9899
z8 12/13	Z	11082	0.02531	0.9856
z9 12/13	Z	10891	-0.02336	0.9993
z10 12/13	Z	10344	0.4515	0.9952
z11 12/13	Z	10685	-2.2363	0.9975
z12 12/13	Z	10705	-2.8614	0.996

Table 4:Calculated Slopes & Intercepts from Objective 1

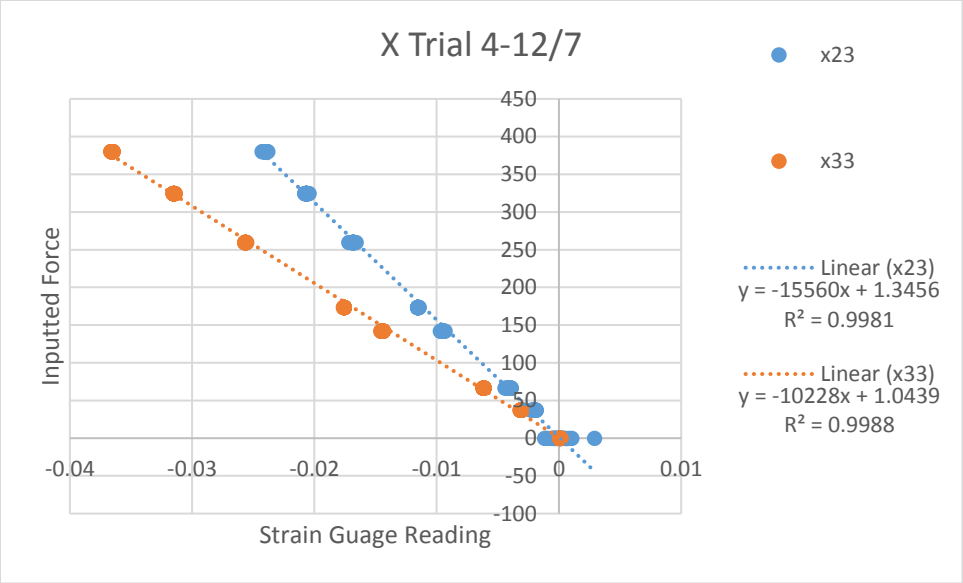

Figure 11: Example Graph and Subsequent Equations Produced form Raw Data

Tables of data for Objective 3

The tables below were developed similarly to the process used in objective 1. The most substantial difference was that the tables below were created from graphs that plotted moments from strain gauges against moments calculated from the fish scale.

	Average	Avedev	ave r^2	Percent Deviation	Percent Error
Xstrain gauge vs fish scale on winch	1.0304	0.005933333	0.998783333	0.58%	3.04%

Ystrain gauge vs fish scale on winch	-0.018183333	0.015188889	0.250916667	-83.53%	
Zstrain gauge vs fish scale on winch	0.752183333	0.002877778	0.998383333	0.38%	0.29%

Table 5: Strain Gauge vs Fish Scale at 750mm

	Average	Avedev	ave r^2	Percent Deviation	Percent Error
xstrain gauge vs fish scale on winch	1.042516667	0.006911111111	0.99925	0.66%	4.25%
ystrain gauge vs fish scale on winch	-0.04093333333	0.02797777778	0.5815666667	-68.35%	
zstrain gauge vs fish scale on winch	0.4426333333	0.004855555556	0.99875	1.10%	-1.64%

Table 6: Strain Gauge vs Fish Scale at 450mm

	Average	Avedev	ave r^2	Percent Deviation	Percent Error
xstrain gauge vs fish scale on winch	1.042133333	0.003755555556	0.9997	0.36%	4.21%
ystrain gauge vs fish scale on winch	-0.07003333333	0.002911111111	0.9697666667	-4.16%	
zstrain gauge vs fish scale on winch	0.1602333333	0.001366666667	0.9978666667	0.85%	-19.88%

Table 7: Strain Gauge vs Fish Scale at 200mm

	Average	Avedev	ave r^2	Percent Deviation	Percent Error
xstrain gauge vs fish scale on winch	1.059516667	0.03018333333	0.9998333333	2.85%	5.95%

ystrain gauge vs fish scale on winch	-0.08988333333	0.007855555556	0.9967	-8.74%	
zstrain gauge vs fish scale on winch	-0.02638333333	0.01081111111	0.9866333333	-40.98%	-2.64%

Table 8: Strain Gauge vs Fish Scale at 0 mm

	Average	Avedev	ave r^2	Percent Deviation	Percent Error
xstrain gauge vs fish scale on winch	1.25408	0.01026	0.99952	0.82%	25.41%
ystrain gauge vs fish scale on winch	-0.19954	0.00293	0.99014	-1.47%	
zstrain gauge vs fish scale on winch	-0.44666	0.00373	0.99898	-0.83%	0.74%

Table 9: Strain Gauge vs Fish Scale at -450mm

	Average	Avedev	ave r^2	Percent Deviation	Percent Error
xstrain gauge vs fish scale on winch	1.40512	0.037856	0.92916	2.69%	40.51%
ystrain gauge vs fish scale on winch	-0.19826	0.127408	0.49796	-64.26%	
zstrain gauge vs fish scale on winch	0.85314	0.017272	0.97346	2.02%	13.75%
ystrain gauge vs fish scale on preload	1.62914	0.604624	0.91536	37.11%	62.91%

Table 10: Strain Gauge vs Fish Scale with Preload at 750mm

	Average	Avedev	ave r^2	Percent Deviation	Percent Error

xstrain gauge vs fish scale on winch	1.241433333	0.0468	0.9644166667	3.77%	24.14%
ystrain gauge vs fish scale on winch	-0.1395333333	0.061	0.6471	-43.72%	
zstrain gauge vs fish scale on winch	0.4976333333	0.01363333333	0.9691	2.74%	10.59%
ystrain gauge vs fish scale on preload	1.16995	0.10115	0.9485	8.65%	17.00%

Table 11: Strain Gauge vs Fish Scale with Preload at 450mm

	Average	Avedev	ave r^2	Percent Deviation	Percent Error
xstrain gauge vs fish scale on winch	0.8566166667	0.07235555556	0.9773	8.45%	-14.34%
ystrain gauge vs fish scale on winch	-0.06876666667	0.04344444444	0.8188166667	-63.18%	
zstrain gauge vs fish scale on winch	0.1373166667	0.01542222222	0.9121333333	11.23%	-31.34%
ystrain gauge vs fish scale on preload	1.388933333	1.094922222	0.9168833333	78.83%	38.89%

Table 12: Strain Gauge vs Fish Scale with Preload at 200mm

	Average	Avedev	ave r^2	Percent Deviation	Percent Error
xstrain gauge vs fish scale on winch	0.97	0.06936666667	0.9794166667	7.15%	-3.00%
ystrain gauge vs	-0.1473166667	0.00435	0.982	-2.95%	

fish scale on winch					
zstrain gauge vs fish scale on winch	0.004733333333	0.009122222222	0.04921666667	192.72%	0.47%
ystrain gauge vs fish scale on preload	4.535316667	3.833916667	0.4726166667	84.53%	353.53%

Table 13: Strain Gauge vs Fish Scale with Preload at 0 mm

	Average	Avedev	ave r^2	Percent Deviation	Percent Error
xstrain gauge vs fish scale on winch	1.365	0.020	0.984	1.44%	36.48%
ystrain gauge vs fish scale on winch	0.062	0.047	0.264	76.80%	
zstrain gauge vs fish scale on winch	-0.037	0.474	0.961	-1283.92%	-108.20%
ystrain gauge vs fish scale on preload	0.165	0.100	0.391	60.69%	-83.49%

Table 14: Strain Gauge vs Fish Scale with Preload at -450mm

APPENDIX II: Build Instructions

General Description

The mechanical system used to build the ski-binding tester consists of a reinforced wooden frame and two pulley systems.

The base of the frame takes the form of an equilateral triangle with a rectangular support that is placed under the triangular frame. On one side of the triangle there is a square wooden frame mounted vertically so a pulley system can be mounted to apply a lateral force on the ski. Directly across from the square frame there is a base for the shaft that will undergo the applied loads of the mechanical system. This base is machined out of steel and allows for a detachable shaft.

The square frame needs to be supported with 2x4 pieces of wood that are cut diagonally and mounted on the rectangular base that sits under the triangular frame. These diagonal pieces of wood ensure that the system does not fold upon itself during testing.

The two pulley systems are used to apply lateral and vertical forces to the ski.

The lateral pulley system consists of a metal bar that is attached at an angle to the square frame (mounted on one side of the equilateral triangle). This metal bar allows for the application of the pulling force at various locations and the angle of the bar is consistent with the angle of the mounted ski. The other part of this system is the wirelessly operated winch that provides the required pulling forces. The winch is mounted on a top corner of the square frame. The winch cable is run through a pulley that is attached at a specified distance on the metal bar, which alters the direction of the pulling force applied by the winch. This wire is then attached to a force gauge (fish scale) that records the pulling force being applied to the ski.

The vertical pulley system consists of a hydraulic system that pulls a wire using applied pressure. The hydraulic system is connected to a pressurized tank that inputs the necessary air pressure using a regulator to produce the required pulling force. The wire is hooked up to two pulleys, one that horizontally guides the wire from the hydraulic system (located under the shaft) to another pulley that guides the wire to the ski. This wire is also connected to a force gauge that shows how much force is being applied to the ski.

All pulling forces are tracked using small cameras and were applied to the ski using moving straps.

Detailed Instructions

Step 1:

Assemble the wooden frame. Start with the square base, then the triangular base that is on top of the square base, then finish the frame with the square frame mounted vertically on one side of the triangular base. Mount the diagonal supports from the square base to the square frame.

Step 2:

Mount the steel base for the shaft. Use wooden supports to get the base at the desired height. Mount the shaft and the ski.

Step 3:

Mount the metal that sits horizontally from shaft base in an orientation that is parallel to the ski. Mount the metal two bars on either side of the shaft base to the square base that is on the floor.

Step 4:

Mount the wirelessly operated winch to the top corner of the square frame. Attach external battery to winch. Assemble the horizontal pulley system by placing the pulley at the designated pull location then run the winch wire through the pulley. Attach a force gauge to the wire.

Step 5:

Mount the hydraulic system under the base of the shaft to the wooden triangular base. Attach the pressurized tank with a regulator to the hydraulic system. Assemble the vertical pulley system by placing the first pulley near the hydraulic system and the second pulley at the designated spot on the metal bars located on the square base. Run a wire through the hydraulic system and both pulleys. Attach a force gauge to the end of the wire.

Step 6:

Mount the moving straps to the ski at the desired location. Secure straps using C-Clamps (Note: If applying force near the bindings, merely use the C-Clamps). Attach the force gauges to the straps or the C-Clamps.

APPENDIX III: Further Work

During this project we developed several uses and modifications that could be done with our testing device in order to analyze different aspects of ski binding performance. The platform that we worked to develop was intended to be flexible and to accommodate many different tests while still maintaining a simple construction.

One of the additional tests we designed the tester to be able to administer was a shock load release test. This shock load test was designed to test skis for inadvertent release due to a sudden vertical load change (slamming action on the ski). This test was planned to be done using the preloading system and a snap shackle to quickly release the load. We planned this test to see if inadvertent release was repeatable at similar load parameters and, if so, what those loads were.

A second test that we planned to test was ski stiffness. We planned to be able to mount a laser tape measurer to the ceiling pointing down on the ski and track the distance the ski moved vs. applied preload using the pneumatic system. This relationship would allow us to measure ski stiffness using our tester.

In addition to these specific tests, there are many other relationships that can be looked at by adding or moving sensors to alternate positons to assess binding performance. The modularity of this system is one of the many benefits that the platform provides.

APPENDIX IV: LabVIEW Explanation

In order to complete our testing, we used a software program called LabVIEW. LabVIEW is a powerful data capture and control software that is used in many different industries. We used the software, paired with a Data Acquisition box (DAQ box) in order to record our data. An image of the DAQ box we used can be seen below in Figure 12.

Figure 12: Image of National Instruments TS, USB 6229 BNC Data Acquisition Box from ES3901 Lab Report.

To have LabVIEW capture and output data we needed to program it to relate the inputs and format the outputs. We programmed it so that it would take the raw data in, offset it by our calibration data, and then output it as moments in the X, Y, and Z orientations. This data was then assigned labels and put into an excel file. The data was only written to this file while button was help on the front panel. The back panel programming is shown below in Figure 13.

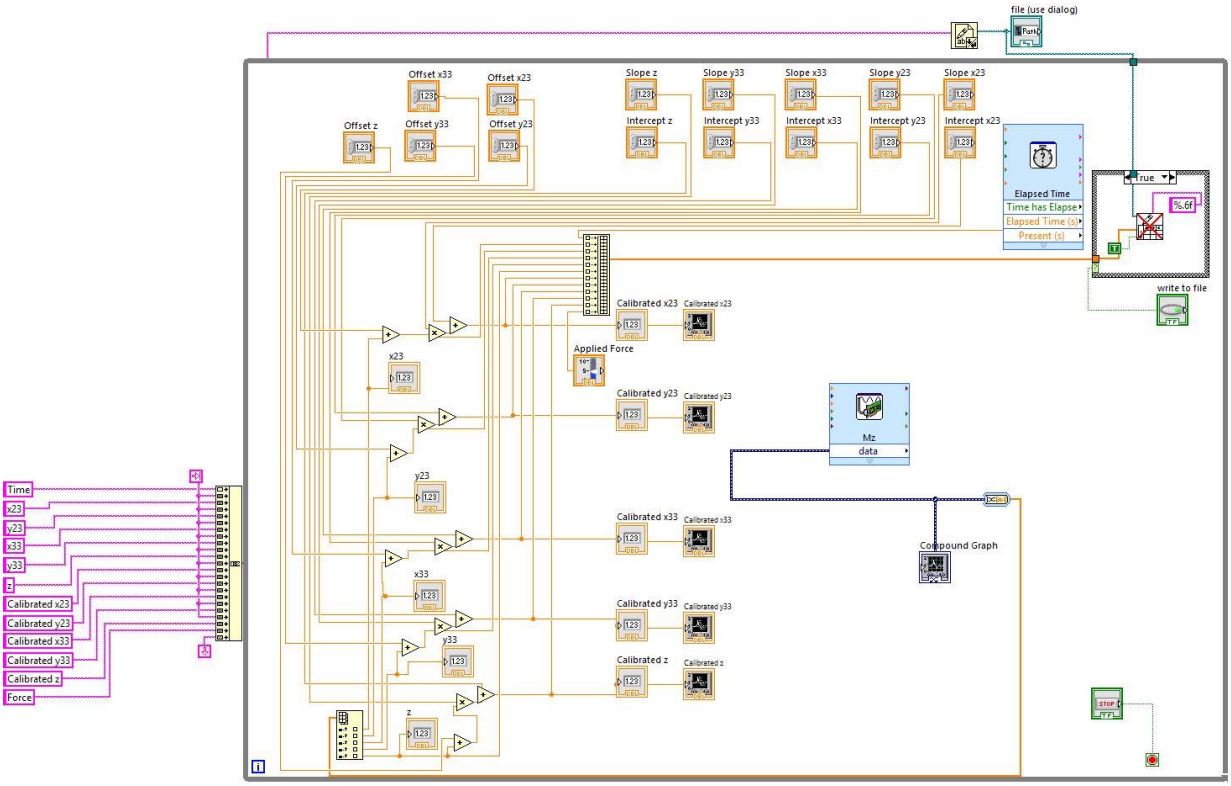

Figure 13: LabVIEW Back Panel

The Front panel is where values and graphs of the data are shown in real-time and where we can control the when the data is recorded. We were also able to change inputs such as the scale reading to simplify later data analyzation. An image of our front panel is shown below in Figure 14 and Figure 15.

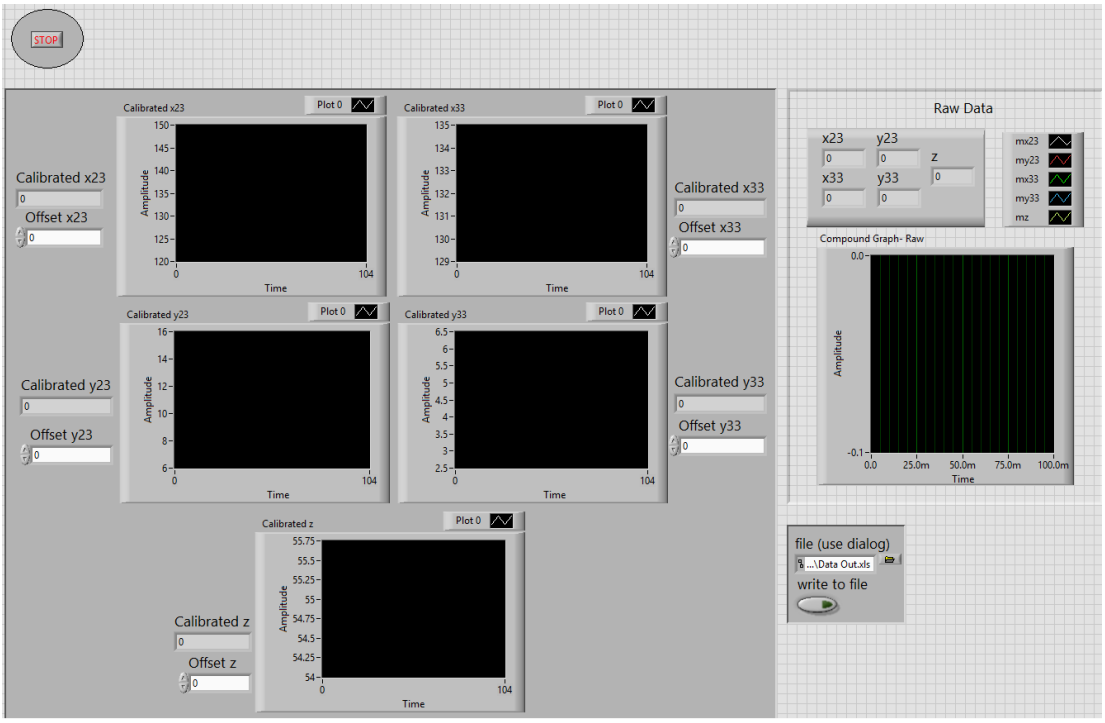

Figure 14: LabVIEW Front Panel 1/2

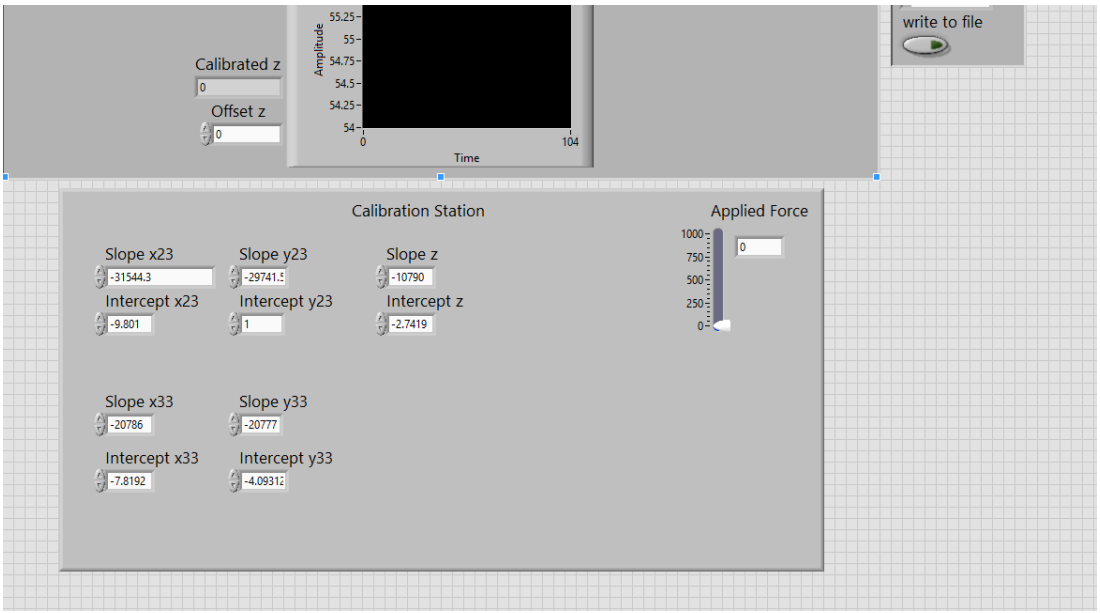

Figure 15: LabVIEW Front Panel 2/2

As you can see in the figures, each set of strain gauges (x23, y23, x33, y33, & z had both an indicator for its value, an offset for calibration, and a graph vs time. The applied force input was where we could write in the force on the scale and it would record it in the data at the correct positions. An example of part of a LabVIEW output file is below in

Figure 16.

Time	x23	y23	x33	y33	z	Calibrate	Calibrate	Calibrate	Calibrate	Calibrated z	Force
1.1009	0.0001	0.0021	0.0001	-6E-05	-0.0002	-1.3414	0.0021	0.0001	-6E-05	-0.0002	0
0.1	0.0002	0.0021	9E-05	-5E-05	-0.0002	-2.722	0.0021	9E-05	-5E-05	-0.0002	0
0.211	5E-05	0.0022	3E-05	-5E-05	-0.0002	-0.6586	0.0022	3E-05	-5E-05	-0.0002	0
0.301	-0.0007	0.0021	8E-05	-6E-05	-0.0002	8.0107	0.0021	8E-05	-6E-05	-0.0002	0
0.4	-0.0002	0.0021	0.0001	-7E-05	-0.0001	1.9244	0.0021	0.0001	-7E-05	-0.0001	0
0.5109	-0.0003	0.0022	8E-05	-6E-05	-0.0002	3.305	0.0022	8E-05	-6E-05	-0.0002	0
0.6109	0.0002	0.0021	0.0001	-3E-05	-0.0002	-2.8259	0.0021	0.0001	-3E-05	-0.0002	0
0.7109	-0.0004	0.0021	8E-05	-2E-05	-0.0002	4.8933	0.0021	8E-05	-2E-05	-0.0002	0
0.8109	0.0002	0.0022	7E-05	-3E-05	-0.0002	-1.9204	0.0022	7E-05	-3E-05	-0.0002	0
0.9109	8E-05	0.0022	0.0001	-6E-05	-0.0002	-0.9852	0.0022	0.0001	-6E-05	-0.0002	0
1.0109	0.0003	0.0022	9E-05	-5E-05	-0.0002	-3.7315	0.0022	9E-05	-5E-05	-0.0002	0
0.101	1E-04	0.0021	8E-05	-8E-05	-0.0002	-1.1633	0.0021	8E-05	-8E-05	-0.0002	0
0.191	0.0003	0.0021	2E-05	-4E-05	-0.0002	-3.776	0.0021	2E-05	-4E-05	-0.0002	0
0.299	-0.0002	0.0021	1E-04	-6E-05	-0.0001	1.8353	0.0021	1E-04	-6E-05	-0.0001	0
0.389	0.0001	0.0022	0.0001	-6E-05	-0.0002	-1.5493	0.0022	0.0001	-6E-05	-0.0002	0
0.489	-0.0002	0.0022	0.0001	-5E-05	-0.0002	1.9244	0.0022	0.0001	-5E-05	-0.0002	0
0.5999	0.0003	0.0022	0.0001	-5E-05	-0.0002	-4.0432	0.0022	0.0001	-5E-05	-0.0002	0
0.7279	4E-06	0.0022	0.0001	-5E-05	-0.0002	-0.05	0.0022	0.0001	-5E-05	-0.0002	0
0.8009	-2E-05	0.0022	1E-04	-4E-05	-0.0002	0.2024	0.0022	1E-04	-4E-05	-0.0002	0
0.8989	9E-05	0.0022	8E-05	-5E-05	-0.0002	-1.0742	0.0022	8E-05	-5E-05	-0.0002	0
0.9989	3E-05	0.0022	8E-05	-5E-05	-0.0002	-0.3468	0.0022	8E-05	-5E-05	-0.0002	0
1.0999	0.0002	0.0022	7E-05	-3E-05	-0.0002	-2.9001	0.0022	7E-05	-3E-05	-0.0002	0
0.091	9E-05	0.0022	1E-04	-7E-05	-0.0002	-1.0891	0.0022	1E-04	-7E-05	-0.0002	0
0.201	-0.0002	0.0022	0.0001	-9E-05	-0.0002	2.0135	0.0022	0.0001	-9E-05	-0.0002	0
0.29	-0.0002	0.0021	1E-04	-5E-05	-0.0002	1.8799	0.0021	1E-04	-5E-05	-0.0002	0
0.389	6E-05	0.0021	7E-05	-4E-05	-0.0002	-0.6883	0.0021	7E-05	-4E-05	-0.0002	0
0.49	-7E-05	0.0022	9E-05	-4E-05	-0.0002	0.8853	0.0022	9E-05	-4E-05	-0.0002	0
0.5889	8E-05	0.0021	0.0001	-7E-05	-0.0002	-0.9406	0.0021	0.0001	-7E-05	-0.0002	0
0.6999	-0.0002	0.0021	6E-05	-7E-05	-0.0002	2.1768	0.0021	6E-05	-7E-05	-0.0002	0
0.7999	7E-05	0.0022	9E-05	-7E-05	-0.0002	-0.8516	0.0022	9E-05	-7E-05	-0.0002	0
0.8999	-0.0003	0.0022	9E-05	-5E-05	-0.0002	3.587	0.0022	9E-05	-5E-05	-0.0002	0
0.9999	0.0003	0.0021	0.0001	-6E-05	-0.0002	-3.3752	0.0021	0.0001	-6E-05	-0.0002	0
1.0929	5E-06	0.0021	0.0001	-0.0001	-0.0002	-0.0648	0.0021	0.0001	-0.0001	-0.0002	0
0.108	0.0001	0.0022	9E-05	-6E-05	-0.0002	-1.8165	0.0022	9E-05	-6E-05	-0.0002	0
0.197	0.0001	0.0022	9E-05	-5E-05	-0.0002	-1.7423	0.0022	9E-05	-5E-05	-0.0002	0
0.308	-0.0006	0.0022	0.0001	-6E-05	-0.0002	7.1943	0.0022	0.0001	-6E-05	-0.0002	0
0.407	0.0004	0.0022	7E-05	-8E-05	-0.0002	-4.6073	0.0022	7E-05	-8E-05	-0.0002	0
0.4	-2E-05	-0.0002	-2E-05	-0.003	-0.0003	0.2024	-0.0002	-2E-05	-0.003	-0.0003	19.6
0.5009	-0.0004	-0.0002	-2E-06	-0.003	-0.0003	5.0715	-0.0002	-2E-06	-0.003	-0.0003	19.6
0.6119	0.0004	-0.0002	-8E-05	-0.003	-0.0003	-4.4588	-0.0002	-8E-05	-0.003	-0.0003	19.6
0.6999	4E-05	-0.0002	-6E-06	-0.003	-0.0003	-0.5101	-0.0002	-6E-06	-0.003	-0.0003	19.6
0.7999	0.0001	-0.0002	-1E-06	-0.003	-0.0003	-1.3266	-0.0002	-1E-06	-0.003	-0.0003	19.6
0.9129	-0.0004	-0.0002	3E-05	-0.0032	-0.0003	4.5519	-0.0002	3E-05	-0.0032	-0.0003	19.6
1.0359	2E-05	-0.0002	-2E-05	-0.0031	-0.0003	-0.2875	-0.0002	-2E-05	-0.0031	-0.0003	19.6
0.077	0.0002	-0.0002	-8E-06	-0.003	-0.0003	-1.8462	-0.0002	-8E-06	-0.003	-0.0003	19.6
0.177	0.0002	-0.0002	-7E-06	-0.003	-0.0003	-3.0041	-0.0002	-7E-06	-0.003	-0.0003	19.6
0.278	0.0002	-0.0002	-2E-05	-0.003	-0.0003	-3.0041	-0.0002	-2E-05	-0.003	-0.0003	19.6
0.376	0.0004	-0.0002	-1E-05	-0.003	-0.0003	-4.6073	-0.0002	-1E-05	-0.003	-0.0003	19.6
0.465	0.0002	-0.0002	-2E-05	-0.003	-0.0003	-2.7962	-0.0002	-2E-05	-0.003	-0.0003	19.6
0.5669	3E-05	-0.0002	-9E-06	-0.003	-0.0002	-0.332	-0.0002	-9E-06	-0.003	-0.0002	19.6
0.6779	-0.0004	-0.0002	-1E-06	-0.003	-0.0003	4.7301	-0.0002	-1E-06	-0.003	-0.0003	19.6
0.7949	1E-04	-0.0002	3E-06	-0.0031	-0.0003	-1.1633	-0.0002	3E-06	-0.0031	-0.0003	19.6
0.8769	0.0003	-0.0002	-3E-05	-0.003	-0.0003	-3.6424	-0.0002	-3E-05	-0.003	-0.0003	19.6
0.9769	4E-05	-0.0002	-7E-05	-0.003	-0.0003	-0.4953	-0.0002	-7E-05	-0.003	-0.0003	19.6
1.0659	8E-05	-0.0002	7E-05	-0.003	-0.0003	-0.9406	-0.0002	7E-05	-0.003	-0.0003	19.6
0.11	0.0001	-0.0002	3E-05	-0.003	-0.0003	-1.5493	-0.0002	3E-05	-0.003	-0.0003	19.6
0.211	6E-05	-0.0002	2E-05	-0.003	-0.0003	-0.7477	-0.0002	2E-05	-0.003	-0.0003	19.6
0.31	-0.0001	-0.0002	3E-06	-0.003	-0.0003	1.583	-0.0002	3E-06	-0.003	-0.0003	19.6
0.399	0.0001	-0.0002	-8E-06	-0.003	-0.0004	-1.7571	-0.0002	-8E-06	-0.003	-0.0004	19.6
0.497	-9E-05	-0.0002	0	-0.003	-0.0003	1.1228	-0.0002	0	-0.003	-0.0003	19.6
0.5979	0.0001	-0.0002	-3E-06	-0.003	-0.0003	-1.5641	-0.0002	-3E-06	-0.003	-0.0003	19.6
0.7129	-0.0002	-0.0002	-7E-06	-0.003	-0.0003	2.3846	-0.0002	-7E-06	-0.003	-0.0003	19.6
0.8159	0.0001	-0.0002	2E-05	-0.003	-0.0003	-1.6235	-0.0002	2E-05	-0.003	-0.0003	19.6
0.9139	-4E-05	-0.0002	2E-05	-0.003	-0.0003	0.4251	-0.0002	2E-05	-0.003	-0.0003	19.6

Figure 16: Example of LabVIEW Output File

APPENDIX V: CAD Drawings

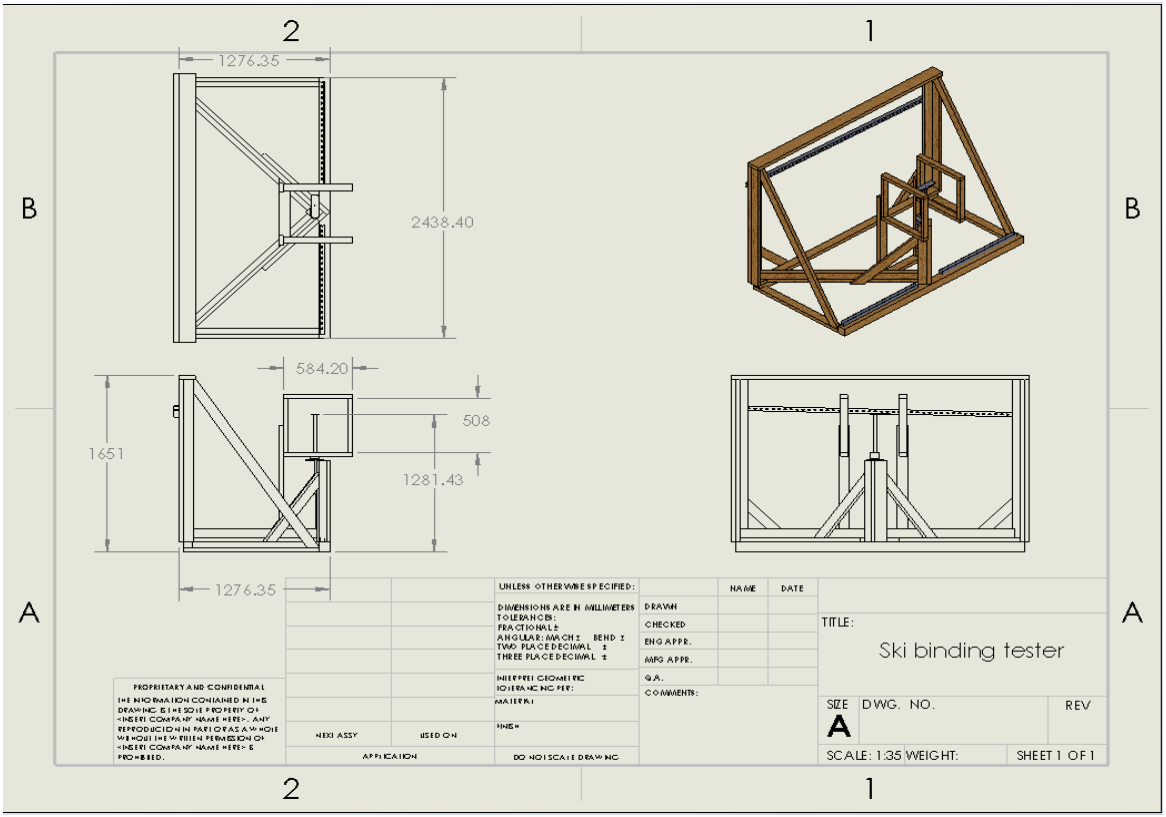

Figure 17: Solidworks Drawing of Ski Binding Tester

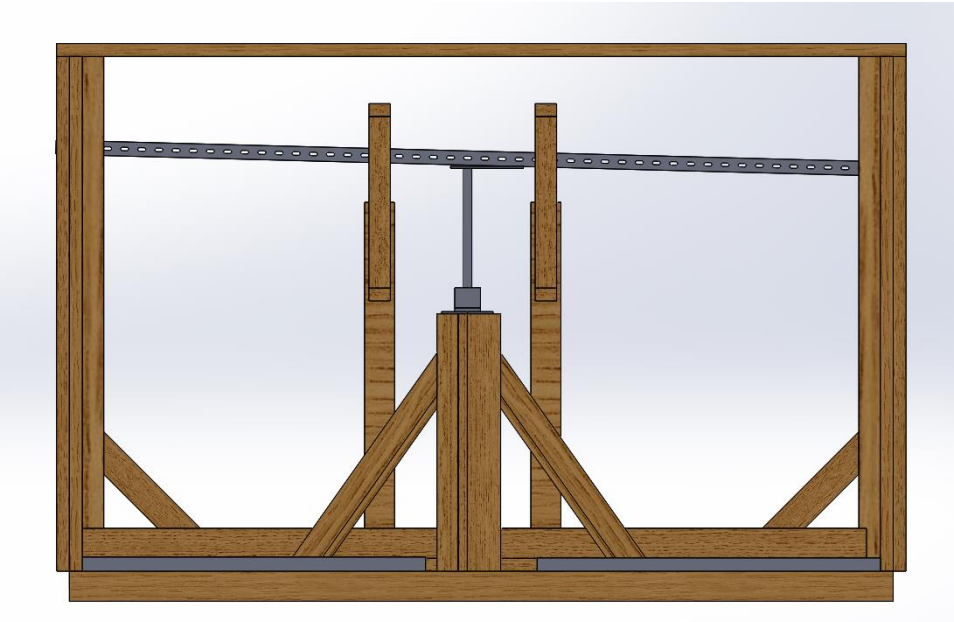

Figure 18: Solidworks Assembly Right View

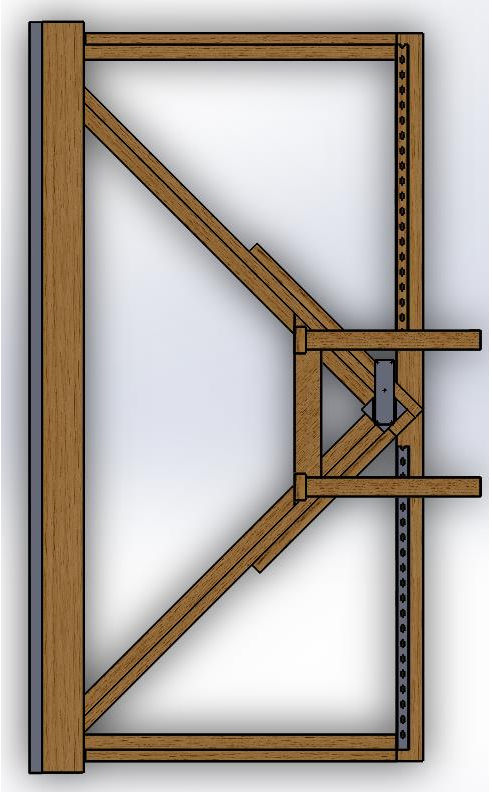

Figure 19: Solidworks Assembly Top View

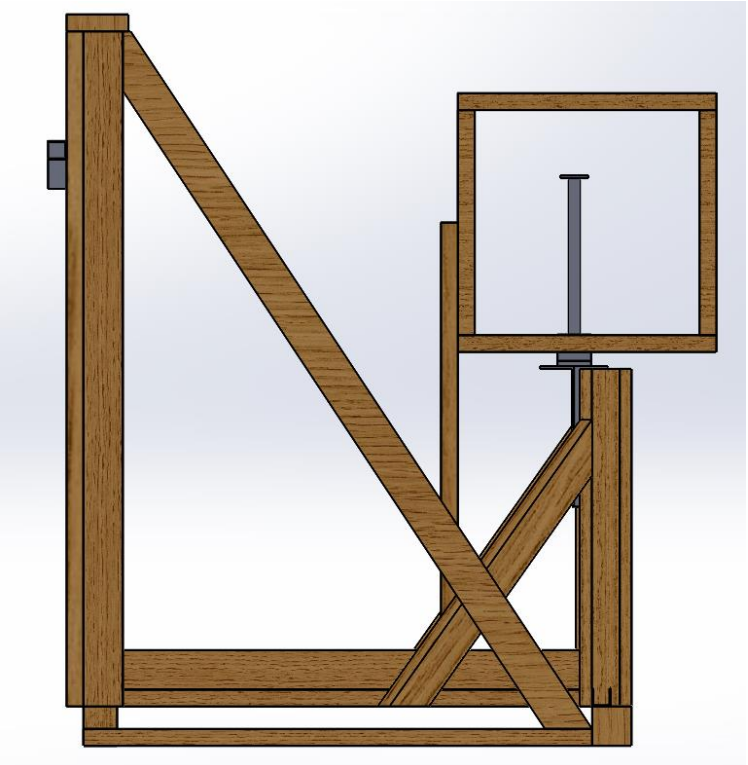

Figure 20: Solidworks Assembly Front View